Electrical machines with switched and modulated flux

Dawid Kara*, Tomasz Kołacz, Jerzy Skwarczyński

University of Applied Sciences in Tarnow, ul. Mickiewicza 8, 33 100 Tarnów, Poland

Abstract

The work compares the value of the produced torque (average value) of a 2.2kW squirrel cage induction motor with new construction machines, i.e. a motor with flux switching and hybrid excitation or DC excited, a motor with flux modulation and hybrid excitation or DC excitation. The external dimensions of the tested machines corresponded to the dimensions of the induction motor.

Keywords: Flux switching machine, hybrid excitation, modulated flux machine, induction motor

Introduction

Over the last 30 years, many new designs for electric machines that are completely different from the traditional ones have been created. The vast majority of these machines have not yet been put into common use despite their creators' assurance about their good unit indicators and performance characteristics. As the choice of the motor type for a specific drive is determined primarily by the value of the torque per unit of volume, the price of its production and exploitation, and reliability, it can be assumed that the new designs are not sufficient competition for those created previously. From the point of view of the theory of electromechanical energy conservation, however, they are very interesting objects due to the original mode of torque generation, short winding overhangs and the simple, practically failure-free rotor structure. Based on the information contained in the available publications, it is difficult to form an objective opinion on the relationship between the commonly used motor and new designs. Therefore, the authors have taken steps in this direction. On the one hand, the choice fell on a low-power squirrel-cage induction motor, and on the other, on those from the new designs that represent the clearest direction of the research. These are machines with reluctance changeable flux direction associated with the armature winding. It seems that among the numerous proposed variants of the aforementioned types of motors, the ones in which the excitation level can be regulated deserve special attention, as this ensures economical operation in conditions of variations in speed over a wide range.

In recent years, there has been an intensification of work on machines without permanent magnets. The expediency of such actions if justified by:
– increasing prices of rare earth magnets,
– limiting their production for objective reasons in the fore-

– seeable time perspective,
– the advantages of being able to adjust the flux level.

Ultimately, a motor with flux switching and hybrid excitation (Hybrid Excitation Flux Switching Machine or HEFSM) and one excited only by the winding (Field Excitation Flux Switching Machine or FEFSM) were selected for comparison. The comparisons were completed with a presentation of properties of the two interesting structures with a modulated stream.

Materials and methods

All of the presented machines were considered as motors powered by three-phase currents from a converter controlled by the rotor position signal. The following formula was used as a basis for the assessment of the produced torque:

$$T_e = \frac{\partial}{\partial \phi}\left(\sum_{n=1}^{N} \psi_{0,n}(\varphi) \cdot i_n\right) = \sum_{n=1}^{N} i_n \frac{\partial \psi_{0,n}(\varphi)}{\partial \varphi} \tag{1}$$

Where:
i_n – the winding currents,
$\psi_{0,n}(\varphi)$ – the fluxes linked with windings in the state of an armature without current,
φ – the rotor position.

The formula essentially applies to machines excited by permanent magnets [1]. It can also be used for machines with an excitation winding, provided that this winding is powered by DC current.

The value calculated according to (1) is the dominant component of the produced moment in most structures, but the others should not be ignored *a priori*. This applied in particular to the so-called cogging torque.

Hybrid excitation flux switching machine

The first design of this type was created at the University of Cachan, France, in 2006 and obtained a patent the following

*Corresponding author: d_kara@pwsztar.edu.pl

www.stijournal.pl

Sci, Tech. Innov 2020; 8 (1), 1-12

year as the Flux-Switching dual-Excitation Electrical Machine [2–4]. It is a complement to the earlier motor concept that lacked a ferromagnetic yoke that mechanically connects individual stator elements [5]. The cross-sections of both machines are shown in Fig. 1.
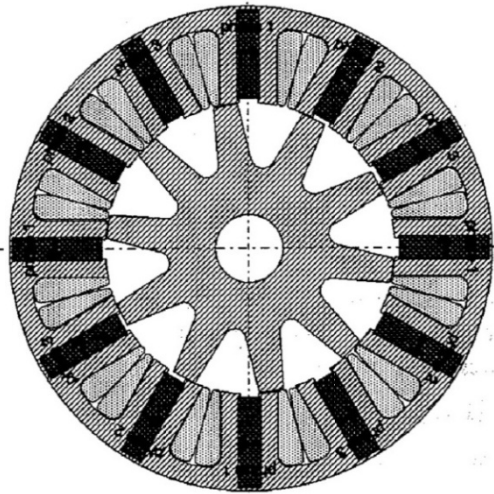
Figure 1a. A motor with flux modulation and permanent magnet excitation [5]
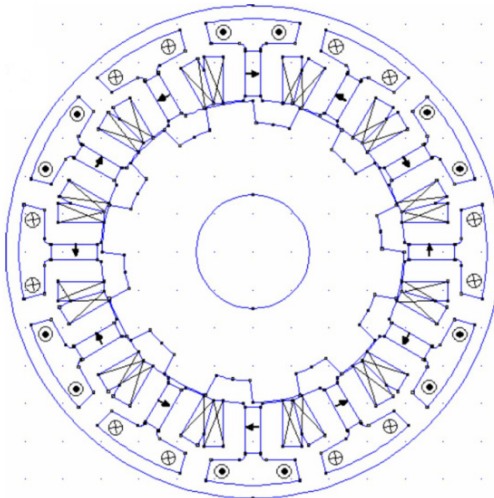
Figure 1b. A motor with flux switching and hybrid excitation [3]

The yoke ring in Fig. 1b creates magnetic bridges for permanent magnets and reduces the generated torque. It makes up the closure of the magnetic circuit for the introduced additional winding, the task of which is to weaken or strengthen the operation of the magnets, depending on the direction of the direct current flowing through the coils. Their operation is schematically explained in Fig. 2.

To achieve effective control of the total excitation flux in the air gap area, the core area around the excitation coils must be properly dimensioned. It is done to reduce the excitation current needed to control the flux, and at the same time not to weaken the action of the magnets too much when the excitation current is not flowing.
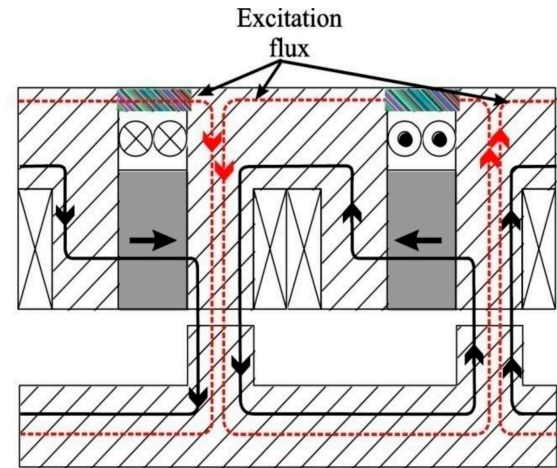
Additional excitation ($J_{exc} > 0$)
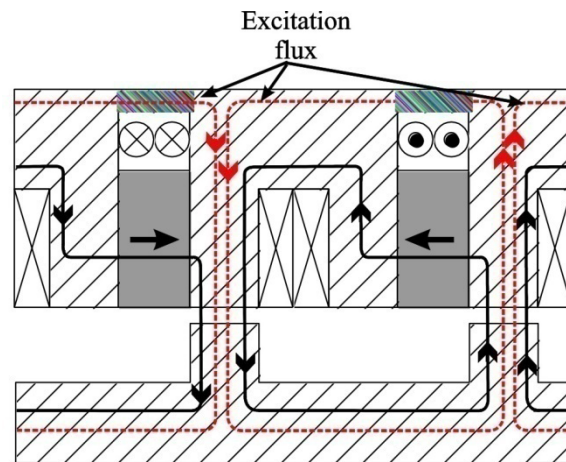
Unexcitation ($J_{exc} < 0$)

Figure 2. The paths of magnetic flux induced by a permanent magnet and excitation coil [4]

The construction gathered great interest in research centres and many of its variants were created. However, all the designs presented so far are not without drawbacks:
– their construction is technologically troublesome,
– permanent magnets are exposed to heating from the windings and the core, and may currently reach temperatures higher than that allowed for them,
– winding faces overlap,
– the complexity of the stator electromagnetic system lowers its reliability.

DC-excited flux-switching machines

In 2010, at a conference in Lille, France[1], and in 2011, at a conference in Birmingham, UK[2], two different teams proposed a way

---

[1] Vehicle Power and Propulsion Conference, Sept. 1–3.

[2] 14th European Conference on Power Electronics and Applications, Aug. 30 – Sept. 1.

to replace permanent magnets with DC coils for three-phase flux-switched motors [6, 7]. The design was a multiplication of the configuration of the excitation and armature windings used in a single-phase AC motor with flux switching [8].

The difference in the construction of the machines with switching flux excited by permanent magnets, as in Fig. 1a, and the excitation winding according to [6] and [7], is well illustrated by the juxtaposition of their coloured cross-sections – Fig. 3 [9].

can be eliminated, while the adjacent (circumferentially) active sides of the coils located closer to the axis of rotation conduct the current in the opposite direction and can be connected frontally to form one turn, as shown in Fig. 4c. The full equivalence of the magnetic circuits from Figs. 4b and 4c cannot be demonstrated analytically, due to the toothing of the air gap edges, the influence of the nonlinearity of the yoke and the share of the leakage flux.

(a) 12/10 FSPMM   (b) 6/8 DCE-FSM
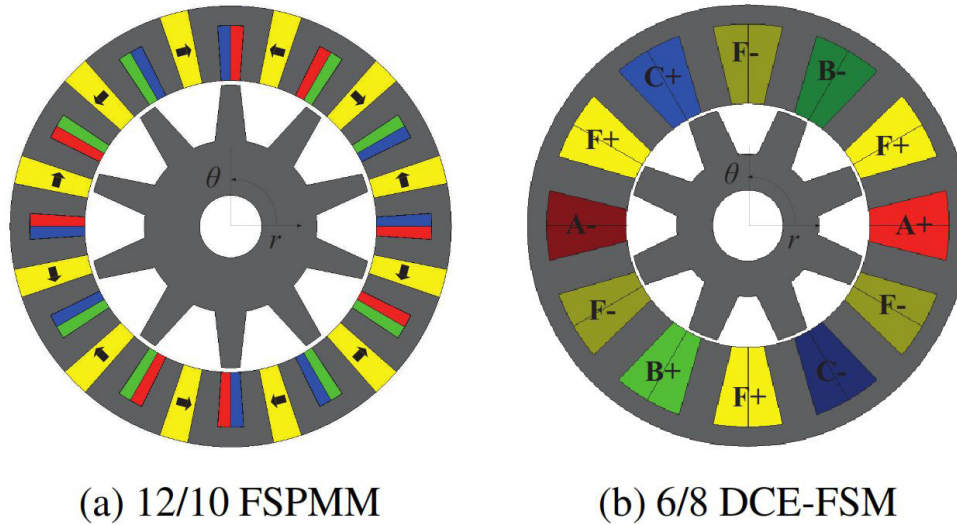
Figure 3. Flux-switching machines with different excitation methods: a) permanent magnet excitation (FSPMM); b) excitation with direct current coils (DCE-FSM) [9]

An intuitive explanation of the equivalence of the design with flux switching, excited by coils and permanent magnets, is provided in [6], which is supported by the cross-sections shown in Fig. 4.It was noticed that the force lines of the field excited by the

Fig. 5 shows fragments of the cross-sections of the new design, taken as the starting point for the optimization process by each of the research teams. Optimization was carried out in terms of obtaining the highest possible moment in the widest

(a)   (b)   (c)
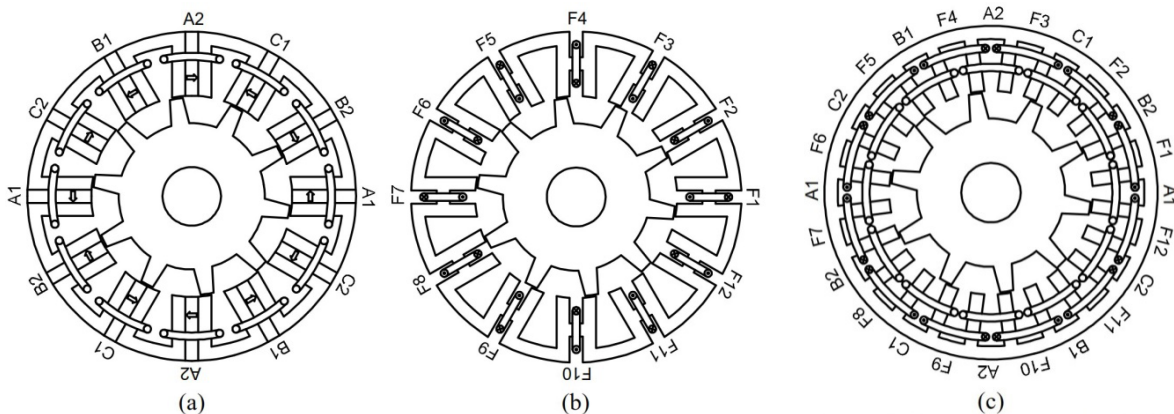
Figure 4. The cross-section of the classic PMFSM – (a), and machines excited by DC windings– (b), (c) [6]

current of the active sides of the turns F1 to F12 in Fig. 4b, located further from the axis of rotation, close outside the stator yoke, don't hit the air gap between the rotor and the stator. These sides

possible range of load changes. As a result, the geometry of the sections changed somewhat, but the end results of the work of the two teams remained different. First of all, the partition coef-

www.stijournal.pl

Sci, Tech. Innov 2020; 8 (1), 1-12
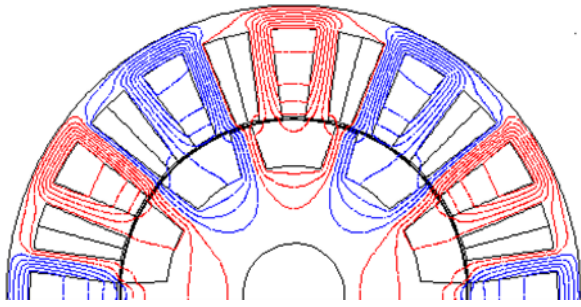
Figure 5a. DCE-FSM according to [6]
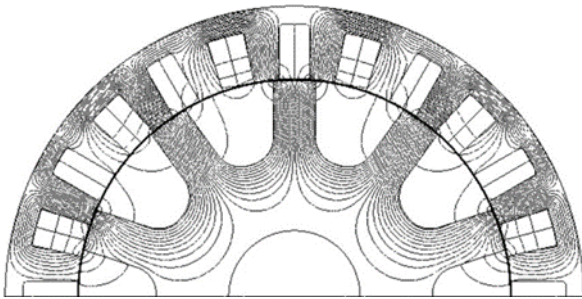
Figure 5b. DCE-FSM according to [7]

ficients[3], considered in [6] as the basic construction parameter, differ in both variants.

In 2013 and 2015, a team from the University of Eindhoven published the results of their own research on FEFSM [9] and their optimization [10] for applications in electric vehicles. It was conducted for the 6 stator teeth/5 rotor pole versions.

The optimal cross-section is shown in Fig. 6. The partition coefficient here is similar to that in the machine in Fig. 5a, but the ratio of the slots area of the armature winding and the excitation is 2:3. This is to ensure the required flow control in the assumed range of rotational speed changes.
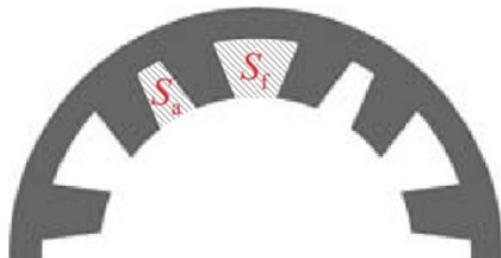
Figure 6. DCE-FSM according to [9]

Opinions about the new design expressed by individual research teams differ. According to [6], the DC-excited FSM, with the same dimensions as PMFSM with neodymium-boron magnets has a much lower torque generation capacity than the PMFSM machine, even when a very high excitation current is

used, which is caused by different magnetic saturation of the winding teeth in both machines. In the FSM machine the teeth are saturated along the entire length, while in the PMFSM only partially. The team from Eindhoven is less critical of FSM [10]: PMFSM can typically provide more torque than DCE-FSM with the same volume. Nevertheless, the DCE-FSM torque density can be increased by minimizing the number of gaps and increasing the ratio between the stator outer diameter and the package length while maintaining the overall machine volume. It is also important that due to the permanent magnets, the temperature in the PMFSM is strictly limited, while the DCE-FSM can operate at higher temperatures, which allows for a higher current density under certain circumstances.

The [7] presents the results of the comparison of the DCE-FSM and IPMSM used in the LEXUS RX400h. Based on the simulation results and laboratory tests, it was found that the final FEFS engine design achieves a power density of 4.8kW/kg, higher than the IM, SRM and IPMSM respectively. The information included in [7] enables the performance of control calculations. They were made in MES-2D using the FEMM program [19]. The results confirmed the results presented in [7], but for a copper slots filling factor of 0.68 and a current density of 21A/mm², which requires cooling the motor with water.

Machines with flux modulation

In machines with flux modulation, the direction of the flux associated with the armature winding does not change. Only its value changes under the influence of the changes in reluctance. Since the SEM induced in the coils depends on the derivative of the flux, the effect of the modulation and diversion is qualitatively similar. Among the many structures whose operation is based on the principle of flux modulation, two will be presented: one with a hybrid excitation system and one excited only with the winding.

Motor with flux modulation and hybrid excitation

The design was classified by its creators as the machines with excitation reversing and named Hybrid Excitation Flux Reversal Machine HE-FRM [11], but with "Flux Reversal" motors it is only connected with the location of the permanent magnets on the stator pole face slot[4]. The cross-section of a typical FRM according to [14] and the HE-FRM according to [11] is shown in Fig. 7.

The possibility of adjusting the excitation flux was obtained by placing different magnets on the adjacent poles (Fig. 7b) instead of the same ones (Fig. 7a). The toothed rotor changes in the HEFRM according to [11] the permeation of the entire pole, not its half, as in the FRM.

---

[3] Partition coefficient (Split Ratio) is the quotient of the inside diameter of the stator yoke to the outside diameter.

[4] The design of the motor with the use of flux reversal was presented in 1996 [11], [12].
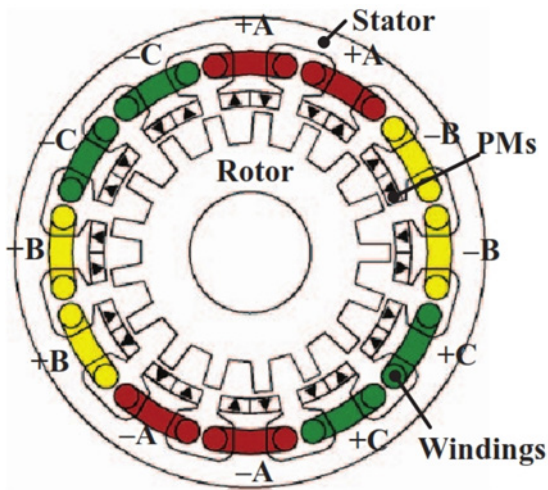
Figure 7a. A typical FRM 12/17 [14]
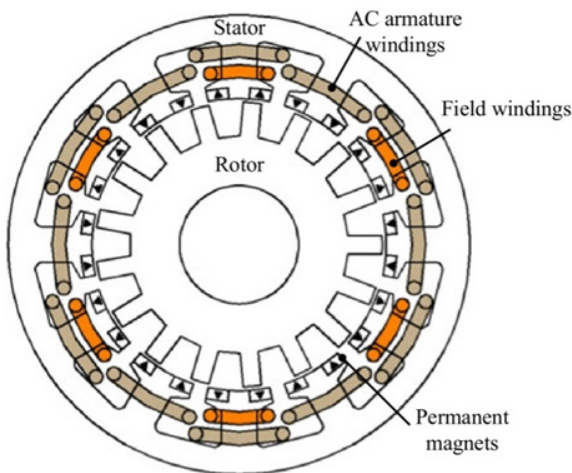
Figure 7b. The HE-FRM [11]

The odd number of the rotor teeth (17) is noticeable. This number provides a relatively high average torque and low pulse, including low cogging torque [15].

According to the conducted analyses, the unbalanced radial force caused by the incomplete symmetry is negligible [16]. However, the problem of elliptical deformation of the stator yoke, caused by the presence of the first harmonic of the field distribution in the air gap, was left open.

It can be seen that for the coils wound around individual teeth, with the orientation as in Fig. 7a, the resultant ampere-turns in every other slot are zero. In the remaining slots, there are ampere-turns from the currents of different phases in the same direction, so the resultant ampere-turns are equal to the ampere turns from the third phase:

$$Ni_A + Ni_B = -Ni_C \qquad (2)$$

The thermal effects of each current are the same if their root mean square (RMS) values are equal. Thus, the Ni_A Ni_B ampere-turns and can be $2Ni_C$ replaced with ampere-turns with the same thermal effect, and twice as much influence on the mag-

netic field, at the same RMS current value. Fig. 8 presents the proposed design changes resulting from the above remarks. The slots in the cross-section in Fig. 8a are not filled with mutually cancelling ampere-turns, but the coil outhangs had to be extended as a result. The area of the cross-section of the empty slots was reduced in size, leaving room for the side of the excitation coil and the ventilation channel (the stator slot fragment without any colour). The information presented in [11] was used to determine the geometry of the stator and rotor gap zone, as well as the partition ratio.
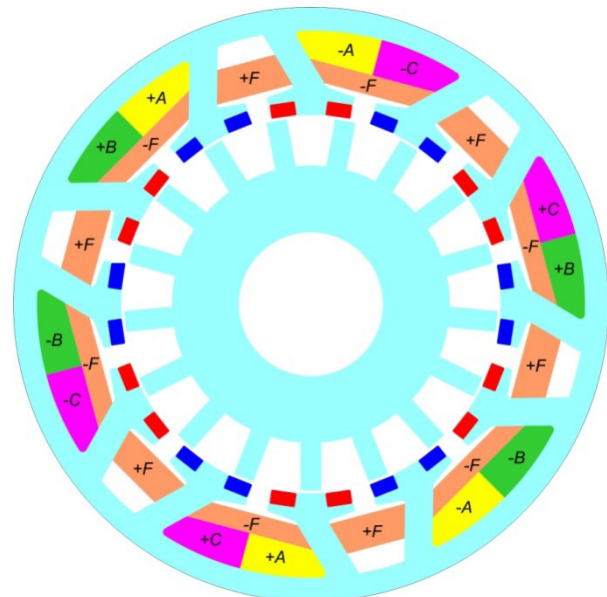
Figure 8a. H-FRM without unnecessary ampere-turns
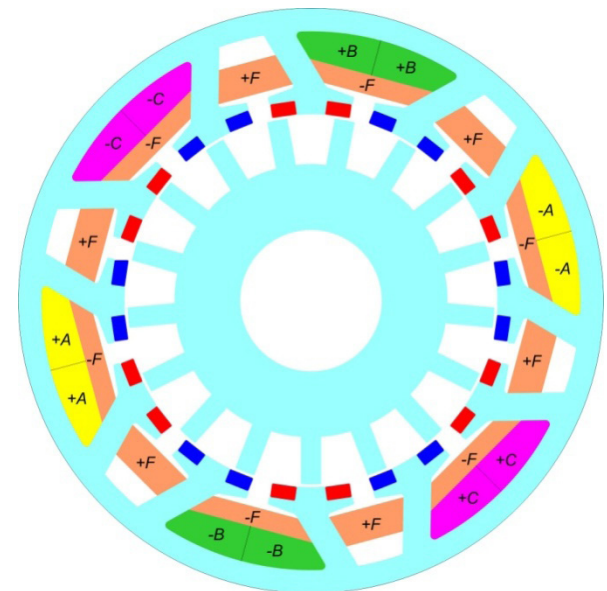
Figure 8b. HE-FRM with long coils overhangs

The structure of the cross-section in Fig. 8b was created as a result of replacing the ampere-turns of two different phases, in the slots of the stator, with the ampere-turns of the third phase, with the sign altered.

www.stijournal.pl

Sci, Tech. Innov 2020; 8 (1), 1-12

The bipolar, three-phase winding now consists of three diameter coils, with their sides overlapping. Such variation provides a torque increase by up to 50%, but the long butt joint connections increase the axial dimension of the motor together with the losses in the windings.

The machine is de facto a Vernier's reluctance reduction motor. It may be referred to as a Hybrid Excited Modulated Flux Machine, HE-MFM.

The motor with flux modulation excited by winding

The originality of the design results from the use of focused coils (around-tooth) in both the excitation winding and the armature, which are located on the same stator teeth. The modulation of the flux with the armature is performed with a toothed rotor – Fig. 9 [17]. Its creators have named the motor a "Low-Speed Multi-Pole Synchronous Machine with a Field Winding on the Stator Side," however, the following name seems more appropriate: DC Excited Modulated Flux Machine, DCE-MFM.
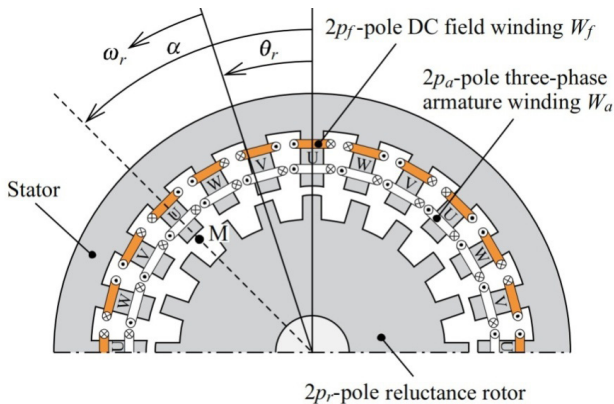
Figure 9. The cross-section of the DCE-MFM [17]

The basic structure of the machine, shown in Fig. 9, has a three-phase armature winding with the number of poles $2p_a = 16$, and an excitation winding with a number of poles $2p_f = 24$. The number of the rotor teeth Z_r must meet the required condition for Dual-Winding Reluctance Machines [18]: $Z_r = (2p_a + 2p_f)/2$. Here $Z_r = 20$. The value $2p_f$ may be the number of stator teeth Z_s. In order to induce three-phase voltages in the armature, such condition should be met: $2pf = K \times 2p_a$, where the coefficient K is $\frac{9}{8}, \frac{6}{5}, \frac{3}{2}$, etc.

The system depicted in Fig. 9 is a fourfold repetition of the basic version $2p_f = 6, 2p_a = 4, Z_r = 5$, which is manifested by four periods of changing fluxes passing through the stator teeth with the rotor doing a full rotation.

When a direct current flows through the excitation winding and the rotor rotates at an angular velocity ω, the EMF period induced in the three-phase armature winding is $1/Z_r$ of a full rotation of the rotor, thus the EMF pulsation is $Z_r \cdot \omega$. At the same time it should also be the pulsation of the three-phase currents in the armature ω_O, which is necessary to

obtain a mean value (other than zero) of the produced torque, according to (1). The armature winding has p_a of pairs of poles, so the rotating field produced by the winding is equal to $\omega_s = \omega_O / p_a = Z_r \omega / p_a$, i.e. $2,5\omega$ for the configurations in question. The rotor rotates in relation to the rotating field with a slip $s = (\omega_s - \omega)/\omega_s = (Z_r - p_a)/Z_r$, which is 0.6 in this case. The possible placement of short circuits in the rotor, e.g. a cage, will result in the generation of additional torque component from the currents induced in the cage.

The creators [18] of the motor calling it "synchronous" came about because, for the armature currents with the pulsation of $\omega_O = Z_r \omega$, the speed of the rotating field of the armature current becomes equal to the speed of the field component originating from the excitation current, which is modulated by the rotor toothing.

Results and Discussion

Formulating the analytical model of the presented structures requires such amount of assumptions and simplifications, that in order to assess their impact on the results, verification of the measurements or field calculations are necessary. For that reason, the evaluation and comparison of the new machines started off with the use of MES, however, it was limited to MES-2D only, as there was an assumption that in all the constructions in question, the axial component of the field is not of high relevance, and therefore can be considered as flat. The calculations were performed in two stages: in the first stage, the associated fluxes of the open windings of the armature, originating from permanent magnets or excitation windings, were determined; in the second stage, the moment developed by an excited motor was determined, with the sinusoidal armature currents remaining in phase with the first harmonic SEM, determined in the first stage. Permanent neodymium-boron magnets with a coercivity intensity of 883,31 kA/m and a relative magnetic permeability of 1.045 were used Br = 1,16 T. The core being non-linear was taken into account.

It was found that, apart from the comparisons between the new designs, it is crucial to compare the results to the appropriate values in traditional motors, especially induction motors. The currently manufactured 2.2kW squirrel cage induction motor was selected for the comparison. For all the machines in comparison, the same dimensions were assumed, as well as the factor of filling the slots with copper (0.35), and the density of the 6.5A/mm2 current, adapted for the induction motor.

The dimensions in question were the ones of a cylinder described on the wound magnetic circuit of the motor, i.e. the outer diameter of the stator package D_z, and the axial dimension of the stator package l_c. The dimension of the stator l_c is greater than the length of the core by itself l_{Fe}, by the total axial dimension of the front joints l_{pcz}: $l_c = l_{Fe} + l_{pcz}$. The value $l_{pcz} = l_{pcz1} + l_{pcz2}$, where the lengths of the fronts on either

side of the machine may usually be considered as similar to each other: $l_{pcz1} \approx l_{pcz2}$. In an induction motor, the value l_{pcz} depends on which winding was used, the number of poles, and the size of the machine, with the ratio of l_c / l_{Fe} being quite wide. Thus, the dimensions of the package of a specific 2.2kW four-pile motor were adapted as reference values: the outer diameter $D_z = 0,152m$, the length of the package l_{Fe} = 0.095m, and the length of the package with winding front connections
$$l_c = 0,095 + 2 \times 0,048 \approx\sim 0,191m .$$

One of the quantities determined by the FEMM program were the streams of the induction vector through a given surface. They are proportional to the vector potential difference at the ends of the trace of a surface on a cross-section of the machine, with the coefficient of proportionality being the side length of the coil, expressed in metres. The determined vector potential differences can, therefore, be deemed as the flux associated to the coil per unit of the axial dimension of that coil, or, in short, the unit flux of the coil. The unit associated fluxes of the coils, determined as the difference in vector potentials in the centres of the geometric sections of the coils, were of particular importance.

1. The motors with flux switching and the hybrid excitation HE-SFM

In order to perform a simulation, the cross-section of the engine presented in [3] – Fig. 1b was used, "photographically" enhanced to a diameter of 0.152m. Their cross-sections are depicted in the figures.

Magnets with a thickness of l_m = 4.07mm, the radial dimension of the air gap between the surfaces of the rotor and stator teeth of δ = 0.22mm, half of the area of the cross-section of the armature of S_t = 71mm², and the area of the cross-section provided for the excitation winding of S_w = 162mm² were adopted.

The average moment according to the MES-2D calculations in FEMM program for l_{Fe} = 0.095m is 14.1Nm for the maximal-ly excited machine. If the butt joints are assumed to be semicircles, their axial dimension is equal to the radius of the largest semicircle and amounts to $l_{pcz} = 2 \times 0,019m$. The dimensions of the induction motor include HE-FSM with a package of length $l_{Feg} = l_c - l_{pcz} = 0,153m$ that can produce a torque of approx. 22.7Nm.

Figures 11 and 12 show the unit flux of the associated armature coils and the developed torque at the rotation of the rotor and maximum excitation. The associated flux of the entire winding (4 coils) changes practically sinusoidally – the greatest harmonics (second and fifth) do not exceed 1.5% and 1% of the fundamental frequency, respectively. The moment changes in the range of the mean value (-0.06; 0.1). The period of the fundamental harmonic is 6 degrees.

2. DCE-FSM DC-excited flux-switching motors

The calculation was done for the combination of 12 stator poles (24 teeth)–10 rotor teeth. The cross-section geometry was selected from several variants compared in terms of the mean and variable moment produced. The cross-section of the motor used in the MES-2D calculations in FEMM is shown in Figure 13.

Radial dimension of the air gap δ = 0.2mm, cross-sectional area of the stator slots S_z = 188mm². The average moment derived from the MES-2D calculations in FEMM program is 13.1Nm for l_{Fe} = 0.095m. If the design version of the end joints is adopted, in which the front joints of the excitation coils are bent and arranged at diameters larger than the front joints of the armature coils, the axial dimension of each armature face must be at least 0.038m. The dimensions of the induction motor then include a DCE-FSM with a package length of $l_{Feg} = 0,191 - 2 \times 0,038 = 0,115m$ that can generate a moment of 15.8Nm.
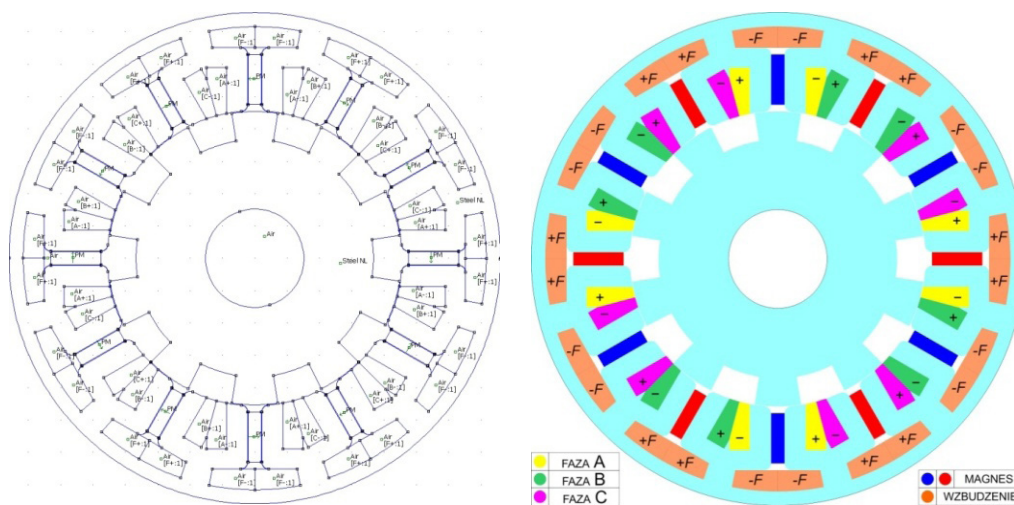
Figure 10. The cross-section of the model intended for calculations with the use of the FEMM program, and the schematic section of HE-FSM
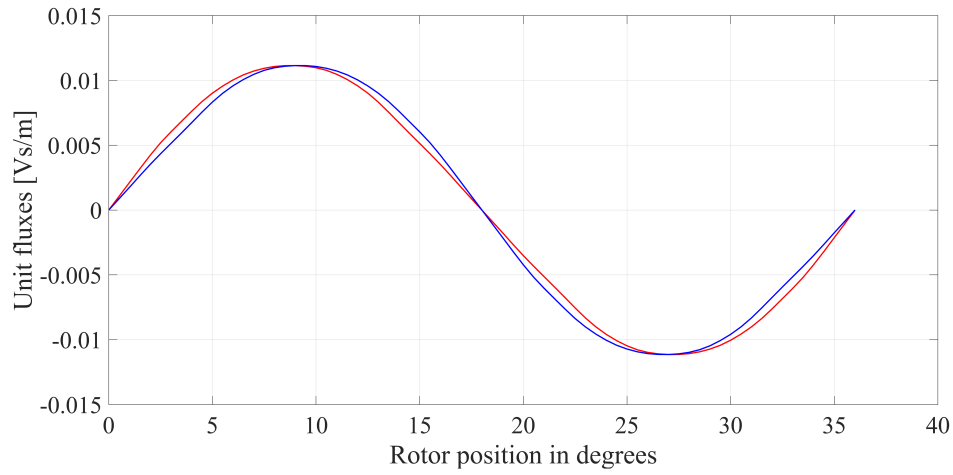
Figure 11. Unit fluxes in armature coils during the rotor's rotation
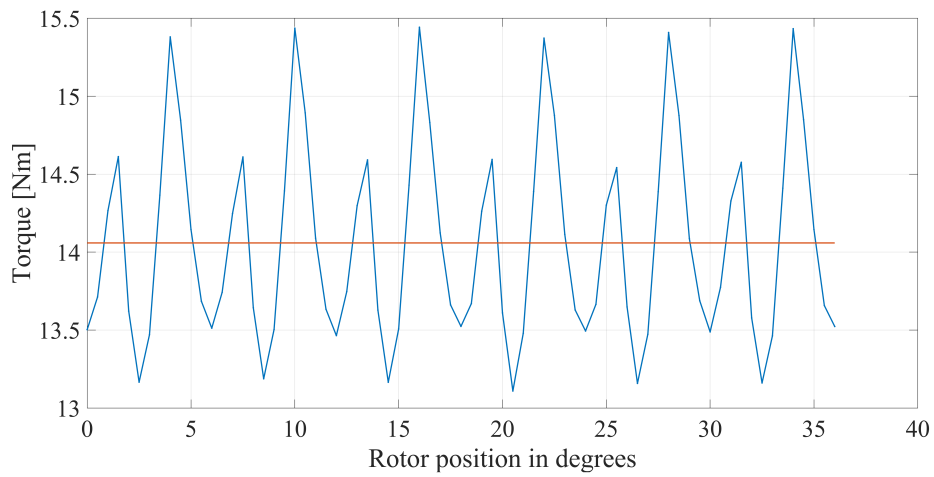
Figure 12. HE-FSM torque during rotor's rotation
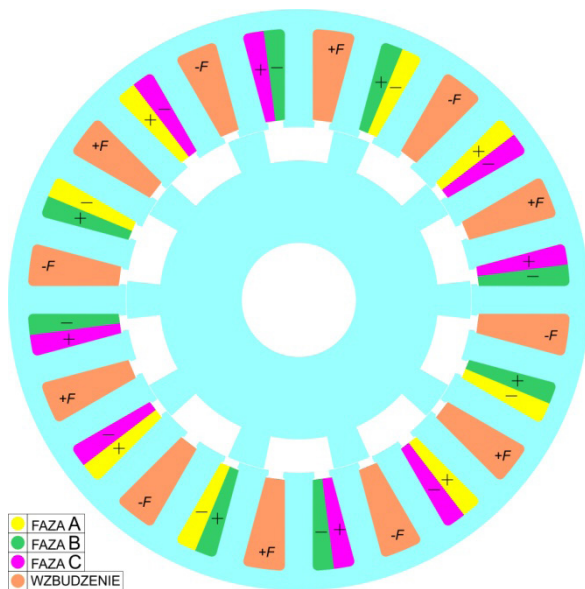
Figure 13. DCE-FSM cross-section
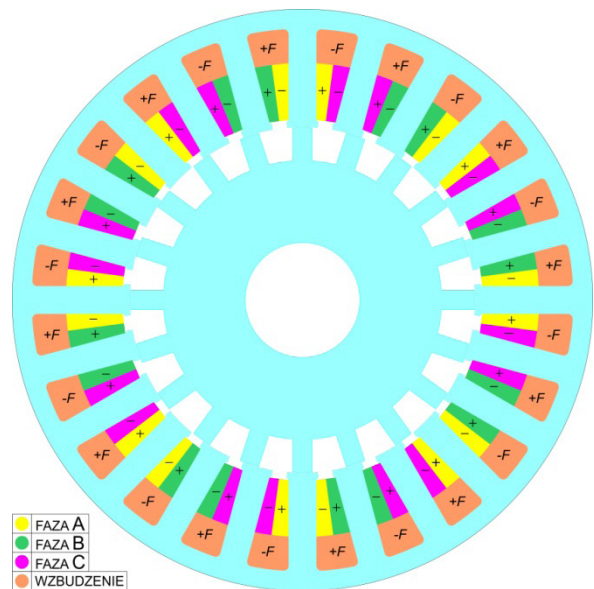
Figure 14. Cross-section of the DCE-MFM

Figures 15 and 16 show the flux unit of the associated armature coils and the torque developed at the rotation of the rotor. The associated flux of the entire winding (4 coils) changes practically sinusoidally—the greatest harmonics (second and fifth) do not exceed 2% and 0.8% of the fundamental frequency, respectively. The moment changes in the range of ±0.08 of the average value. The period of the fundamental harmonic is 6 degrees.

for the diameter windings (as in Fig. 8b). The span of the coil outhangs is similar to that of an induction motor and maintaining the dimensions does not allow for the package extension. On the other hand, 6 ventilation channels enable the increase of the current density and the generated torque in both variants.

The associated flux of the winding diameter turns is practically sinusoidal – the greatest harmonics (second and third)
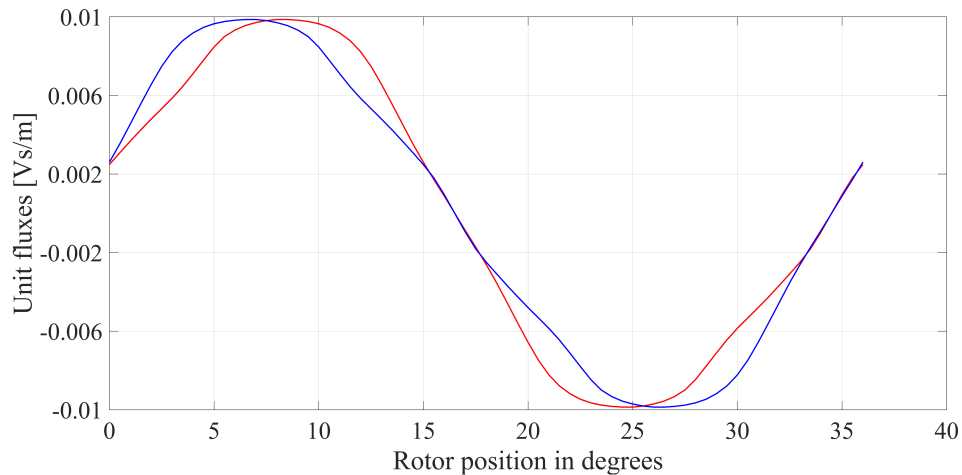
Figure 15. Unit fluxes in armature coils during the rotation of the rotor
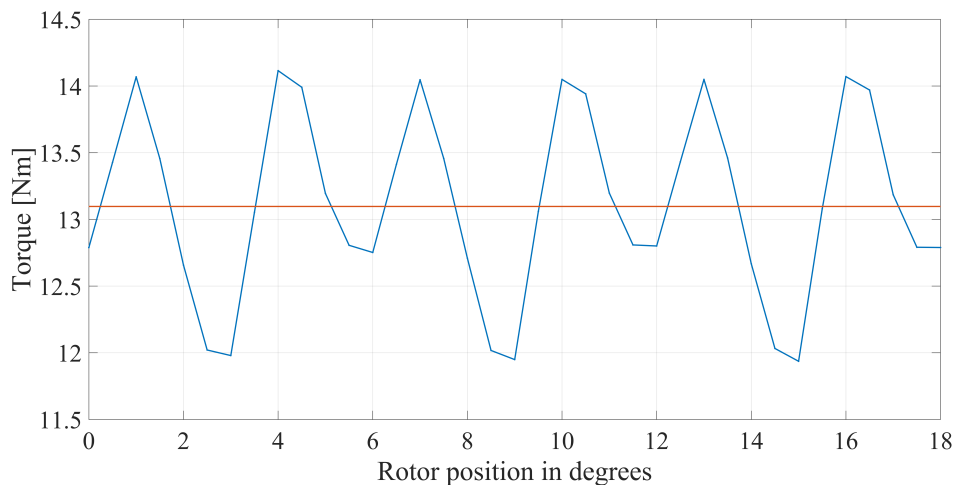
Figure 16. DCE-FSM torque during the rotation of the rotor

3. Motors with flux modulation and HE-MSM hybrid excitation

In the calculations made in FEMM, the cross-sections of the motors presented in Figures 8a and 8b were used. The thickness of the magnet was $l_m = 3.56$mm. The air gap was $\delta = 0.73$mm, the cross-section area of the stator slot provided for the armature winding $S_t = 150$mm², the section area of the stator slot provided for the excitation winding $S_w = 135$mm². For the yoke $l_{Fe} = 0.095$m long, the mean moment calculated by FEMM program is 8.9Nm for the shortened windings (as in Fig. 8a) and 12.5Nm

do not exceed 2% of the fundamental frequency. The moment changes in the range ±0.03 of the mean value, so less than for the machines presented earlier. The period of the fundamental harmonic of the torque variable component is close to 3.5 degrees (60/17).

4. Motors with flux modulation excited by DCE-MFM winding

The shape of the stator plates identical to that of the DCE-FSM motor was used in computer simulations (Fig. 13). The radial di-

mension of the gap δ = 0.2mm was also left unchanged. Stator slots cross-sectional area is S_z = 188mm² (as in DCE-FSM). The area of the cross-section of the stator slot part provided for the armature winding is S_t = 47mm², and the cross-sectional area of the stator slot part provided for the excitation winding S_w = 94mm². For the yoke with the length of l_{Fe} = 0.095 m, the mean moment calculated by FEMM program is 6.4*Nm*. The design of the DCE-MFM as shown in Fig. 14 provides very short coil outhangs that only extend the yoke by $2 \times 0,01 m$. Keeping the dimensions, the length of the package can be increased to the value of $l_{Feg} = 0,191 - 2 \times 0,01 = 0,171 m$. The produced torque is then 11.5Nm.

Figure 17 shows the unit flux of the associated armature coils (red and blue lines) and the entire winding of one phase (8 coils) in black. The unidirectional nature of the flux of the associated coils is visible. The associated flux of the entire winding already resembles a sine wave, but the harmonic content is slightly higher than before: the largest (second) harmonic reaches 3.5% of the fundamental frequency, the third 2%, and the fourth 1.5%. The others do not exceed 1%. Figure 18 shows the changes in the developed torque during the rotation of the rotor. The moment varies within the range of (-0.06; 0.11) of the mean value. The period of the fundamental harmonic is 3 degrees.

Conclusions

The table compares the calculated values of the torque developed by the presented structures with the torque developed by the low-power squirrel-cage induction motor. The external dimensions of the tested machines corresponded to the dimensions of the induction motor. The slot filling factor and the current density in the windings are also maintained, although the rotor without windings allows increasing heat generation in the stator.

The values presented in the table show that in the yokes with the same external dimensions, the highest torque is generated in the induction motor. The torque value in HE-FSM is smaller but similar. This value increases by over 50% when the dimensions of the motor are enlarged to the dimensions of the induction motor. However, lengthening the yoke at the expense of the butt joints will increase the weight of the motor. On the other hand, by far the smallest moment is generated in the DCE-MFM. This engine has very short, non-overlapping coil outhangs.

The obtained results allow only for the assessment of the ability to generate torque in various electromagnetic systems with similar dimensions. This caution in formulating opinions results from the significant influence of the size of the butt joints on
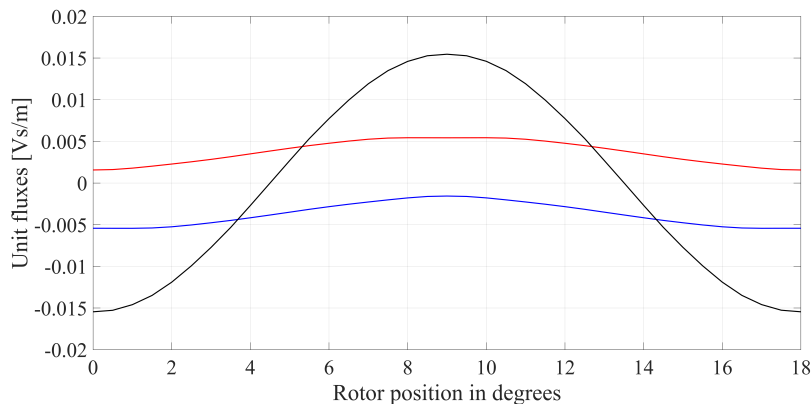
Figure 17. Unit fluxes in coils and armature winding at the rotation of the rotor
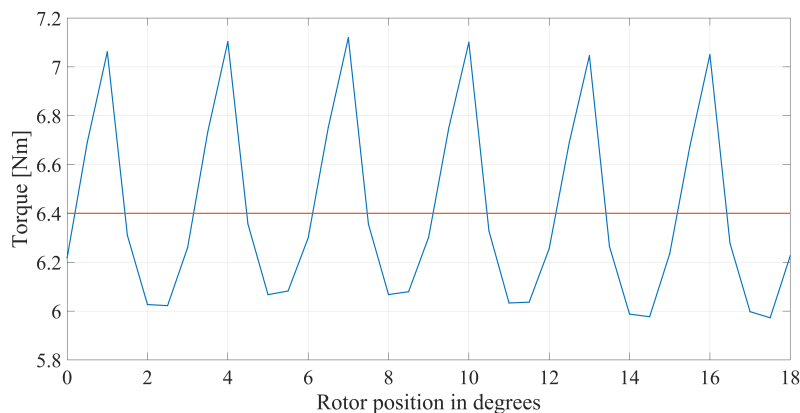
Figure 18. DCE-MFM torque during the rotation of the rotor

Table 1. The comparison of the magnitude of the torque developed by the motors

	Induction motor	HE-FSM	DCE-FSM	HE-MFM	DCE-MFM
T_{sr} [Nm] for l_{Fe} =0.095m	14,6 (1435 rpm)	14.1	13.1	12.5	6.4
T_{sr} [Nm] for l_{Feg}	-	22.7	15.8	-	11.5
T_{zm} [% T_{sr}]	-	− 6, +10	± 8	± 3	− 6, +11

the projected value of the produced torque per unit of volume. It should be remembered that the considered induction motor was created as a result of many years of experience and optimization procedures, which the presented new machines are devoid of.

In our opinion, the DCE-FSM motor deserves special attention due to its very simple structure without expensive permanent magnets, and due to being able to produce a torque comparable to that of an induction motor, but practically independent of the speed. Obviously, the magnitude of the produced torque per unit of volume does not determine the operational properties of the engine. Therefore, the new design of the DCE-FSM is still subject to extensive testing.

Acknowledgements

Author Contributions

Conceptualization, Skwarczyński J. and Kołacz T.; methodology, Skwarczyński J.; software, Skwarczyński J.; validation, Skwarczyński J. and Kara D.; formal analysis, Skwarczyński J.; investigation, Kołacz T.; resources, Skwarczyński J. and Kara D.; data curation, Kara D.; writing – original draft preparation, Kara D.; writing – review and editing, Kołacz T.; visualization, Kara D.; supervision, Kołacz T. and Kara D.; project administration, Skwarczyński J.; funding acquisition, Skwarczyński J.

References

1. Sobczyk TJ. Problemy modelowania matematycznego prądnic synchronicznych wzbudzanych magnesami trwałymi. Prace instytutu elektrotechniki. 2007;231:99-123.

2. Hoang E, Lecrivain M, Gabsi M, inventors. CNRS, assignee. Machine *électrique* a commutation de flux et a double excitation. International Patent FR0602058. 2007-03-08.

3. Hoang E, Lecrivain M, Gabsi M.A new structure of a switching flux synchronous polyphased machine with hybrid excitation. Proceedings of the2007 European Conference on Power Electronics and Applications; 2007 Sep 2-5; Aalbork, Denmark. IEEE; 2008, pp. 1–8. doi: https://doi.org/10.1109/EPE.2007.4417204.

4. Hoang E, Lécrivain M, Hlioui S, Gabsi M. Hybrid excitation synchronous permanent magnets synchronous machines optimally designed for hybrid and full electrical vehicle. Proceedings of the 8th International Conference on Power Electronics – ECCE Asia; 2011 May 30 – Jun 3; Jeju, South Korea. IEEE; 2011, pp. 153–160. doi: https://doi.org/10.1109/ICPE.2011.5944569.

5. Hoang E, Ben-Ahmed AH, Lucidarme J. Switching flux permanent magnet polyphased synchronous machines. Proceedings of the 7th European Conference on Power Electron Application; 1997 Sep 8-10; Trondheim, Norway. EPE Association; 1997, vol. 3, pp. 903–908.

6. Chen JT, Zhu ZQ,Iwasaki S, Deodhar R. Low Cost Flux-Switching Brushless AC Machines. Proceedings of the 2010 IEEE Vehicle Power and Propulsion Conference; 2010 Sep 1-3; Lille, France. IEEE; 2011, pp. 1–6. doi: https://doi.org/10.1109/VPPC.2010.5728984.

7. Sulaiman E, Kosaka T, Matsui N. A new structure of 12Slot-10Pole field-excitation flux switching synchronous machine for hybrid electric vehicles. Proceedings of the 2011 14th European Conference on Power Electronics and Applications; 2011 Aug 30 – Sep 1; Birmingham, UK. IEEE; 2011, pp. 1–10.

8. Pollock C,Wallace M.The flux switching motor, a DC motor without magnets or brushes. Conference Record of the 1999 IEEE Industry Applications Conference. Thirty-Forth IAS Annual Meeting (Cat. No.99CH36370); 1999 Oct 3-7; Phoenix, AZ, USA. IEEE; 2002, vol.3, pp.1980-1987. doi: https://doi.org/10.1109/IAS.1999.806009.

9. Tang Y, Ilhan E, Paulides JJH, Lomonova EA. Design considerations of flux-switching machines with permanent magnet or DC excitation. Proceedings of the2013 15th European Conference on Power Electronics and Applications (EPE); 2013 Sep 2-6; Lille, France. IEEE; 2013, pp. 1–10. doi: https://doi.org/10.1109/EPE.2013.6634396.

10. Tang Y, Paulides JJH, Lomonova EA. Field weakening performance of flux-switching machines for hybrid/electric vehicles. Proceedings of the 2015-Tenth International Conference on Ecological Vehicles and Renewable Energies (EVER), 2015 Mar 31 – Apr 2; Monte Carlo, Monaco. IEEE; 2015, pp. 1-10. doi: https://doi.org/10.1109/EVER.2015.7112995.

11. Gao Y, Qu R, Li D, Li J. A Novel Hybrid Excitation Flux Reversal Machine for Electric Vehicle Propulsion. Proceedings of the 13th IEEE Vehicle Power and Propulsion Conference (VPPC); 2016Oct 17-20; Hangzhou, China. IEEE; 2016, pp. 1–6. doi: https://doi.org/10.1109/VPPC.2016.7791585.

12. Boldea I, Serban E, Babau R. Flux reversal stator-PM single-phase generator with controlled DC output. Record of OPTIM-96; 1996 May; Brasov, Romania. pp. 1123-1137.

13. Deodhar RP, Andersson S, Boldea I, Miller TJE. The flux-reversal machine: anew brushless doubly-salient permanent-magnet machine. IAS '96. Conference Record of the 1996 IEEE Industry Applications Conference Thirty-First IAS Annual Meeting; 1996 Oct 6-10; San Diego, CA, USA. IEEE; 2002, vol. 2, pp. 786 – 793. doi: https://doi.org/10.1109/IAS.1996.560174.

14. Gao Y, Qu R, Li D, Li J. Design and comparison of novel flux reversal machines with large stator slot opening. Proceedings of the2016 IEEE Conference on Electromagnetic Field Computation (CEFC); 2016 Nov 13-16; Miami, FL, USA. IEEE; 2017, pp. 1-1. doi: https://doi.org/10.1109/CEFC.2016.7816195.

15. Gao Y, Qu R, Li D, Li J. Design procedure of flux reversal permanent magnet machines. Proceedings of the 2016 XXII International Conference on Electrical Machines (ICEM); 2016 Sep 4-7; Lausanne, Switzerland. IEEE; 2016, pp. 1584–1590. doi: https://doi.org/10.1109/ICELMACH.2016.7732735.

16. Gao Y, Li D, Qu R, Li J. Design procedure of flux reversal permanent magnet machines. IEEE Transactions on Industry Applications. 2017;53(5):4232–4241. doi: https://doi.org/10.1109/TIA.2017.2695980.

17. Fukami T, Matsuura Y, Shima K, Momiyama M, Kawamura M. Development of a low-speed multi-pole synchronous machine with a field winding on the stator side. Proceedings of the XIX International Conference on Electrical Machines - ICEM 2010; 2010 Sep 6-8; Rome, Italy. IEEE; 2010, pp. 1-6, doi: https://doi.org/10.1109/ICELMACH.2010.5608212.

18. Fukami T, Momiyama M, Shima K, Hanaoka R, Takata S. Steady-State Analysis of a Dual-Winding Reluctance Generator With a Multiple-Barrier Rotor. IEEE Transactions on Energy Conversion. 2008;23(2):492–498. doi: https://doi.org/10.1109/TEC.2008.918656.

19. http://www.femm.info/wiki/HomePage.